Bone-targeting phospholipid polymers to solubilize the lipophilic anticancer drug

Akihisa OTAKA[a], Tomoki YAMAGUCHI[b], Ryoya SAISHO[b], Toru HIRAGA[c], and Yasuhiko IWASAKI[a, b]*

a ORDIST, Kansai University, 3-3-35 Yamate-cho, Suita-shi, Osaka, 564-8680, Japan

b Department of Chemistry and Materials Engineering Faculty of Chemistry, Materials and Bioengineering, 3-3-35 Yamate-cho, Suita-shi, Osaka, 564-8680, Japan

c Department of Histology and Cell Biology, Matsumoto Dental University, 1780 Gobara Hirooka, Shiojiri-shi, Nagano, 399-0781, JAPAN

E-mail: yasu.bmt@kansai-u.ac.jp

ABSTRACT

Current chemotherapy methods have limited effectiveness in eliminating bone metastasis, which leads to a poor prognosis associated with severe bone disorders. To provide regional chemotherapy for this metastatic tumor, a bone-targeting drug carrier was produced by introducing the osteotropic bisphosphonate alendronate (ALN) units into an amphiphilic phospholipid polymer, poly(2-methacryloyloxyethyl phosphorylcholine-*co*-*n*-butyl methacrylate). The polymer can form nanoparticles with a diameter of less than 30 nm; ALN units were exposed to the outer layer of the particle. A simple mixing procedure was used to encapsulate a hydrophobic anticancer drug, known as docetaxel (DTX), in the polymer nanoparticle, providing a uniform solution of a polymer-DTX complex in the aqueous phase. The complex showed anticancer activities against several breast cancer cell lines, and the complex formation did not hamper the pharmacological effect of DTX. The fluorescence observations evaluated by an *in vivo* imaging system and fluorescence microscopy showed that the addition of ALN to the polymer-DTX complex enhanced bone accumulation. Bone-targeting phospholipid polymers are potential solubilizing

excipients used to formulate DTX and deliver the hydrophobic drug to bone tissues by blood administration.

KEYWORDS

bone metastasis, 2-methacryloyloxyethyl phosphorylcholine, alendronate, docetaxel, breast cancer cell

1. INTRODUCTION

Breast, lung, and prostate cancers account for approximately one third of neoplasm mortality.[1] Their cumulative annual incidence is approximately 290,000 patients in Japan[1] and more than 5 million worldwide.[2] These cancers tend to invade bone marrow via the circulatory system in a high incidence rate from 19% to 65%,[3] leading to a poor prognosis associated with serious complications such as pathological fractures, hypercalcemia and bone pain.[4] Taxoid drugs are widely used antineoplastic agents for metastatic breast[5] or prostate cancers.[6] Current systemic chemotherapy methods have limited effectiveness in eliminating bone-residing tumors.[7],[8] While a dose increase can somewhat provide clinical responses in the suppression of bone metastasis,[9] high-dose chemotherapy, owing to systemic adverse effects, is still not recommended because of its weak survival records and poor improvement to the quality of life.[9],[10] Hence, regional chemotherapy has the potential to achieve localized antineoplastic effects in bone-metastatic sites and decrease systemic side effects.[11]

In the past few decades, there has been a growing interest in polymers as drug

delivery systems for skeletal disorders.[11]–[17] For example, bone-targeting polymer nanoparticles (NPs), composed of block copolymers of poly(D,L-lactide-*co*-glycolide) (PLGA) and polyethylene glycol (PEG) with bisphosphonate (BP) residues, have been proposed as bone-targeting drug carriers.[17] Some research groups have reported that the drug-embedded NPs can inhibit myeloma progression in mice.[15] *N*-(2-hydroxypropyl)methacrylamide (HPMA) polymer, conjugated with bone-targeting pendant groups, is another polymeric carrier for bone-targeting drug delivery,[18] and the drugs conjugated with HPMA have been reported to suppress the progression of bone metastases.[11],[13] In the studies noted above, hydrophilic polymers play critical roles in offering extended circulating half-lives of polymer-drug complexes, minimizing the clearance of loaded drugs and conferring reactive sites to immobilize bone-targeting moieties in the complex.[3],[19] However, PEG is reported to induce an accelerated blood clearance (ABC), in which initially administered nanocarriers induce humoral immunity by producing immunoglobulin (e.g., anti-PEG antibody), resulting in diseased circulating half-lives in the subsequent administration.[20],[21] Therefore, improving antifouling property of polymers is still in great demand for elongating blood retention.

2-Methacryloyloxyethyl phosphorylcholine (MPC) is one of the biocompatible

monomers bearing the zwitterionic phosphorylcholine group, that offers a hydrophilic interface resisting opsonization and protein adsorption.[22] For example, a microsphere with an MPC moiety on its surface have been reported to suppress the adsorption of albumin and globulin compared with a microsphere with an HPMA polymer surface.[23] Even more, the phosphorylcholine group in the MPC moiety has also been reported not to induce the ABC, unlike PEGylated materials.[20] Since repeated administrations are conducted in cancer chemotherapy, the MPC-bearing drug carrier seems to be more applicable.[24],[25] The copolymers of MPC and *n*-butyl methacrylate (BMA) (PMB) form self-assembly nanospheres in water, offering a blood-compatible hydrophilic shell and a hydrophobic pocket.[26] Previous researches have reported the successful performing of the formulations of the paclitaxel embedded in the PMB[27] with the complex exerting an antineoplastic effect on hepatocellular, squamous cell,[28] gastric,[29] and bladder carcinomas.[30]

Bioactive groups, such as oligopeptides,[31] ligands,[28],[32] and antibodies[33],[34] were introduced to carry out the target-specific functionalization of PMB. However, to the best of our knowledge, no studies have to date focused on bone-targeting phospholipid polymers. In this study, amphiphilic phospholipid polymers, endowed with an osteotropic alendronate (ALN) moiety, a class of nitrogen-containing BP

compounds, were synthesized; their drug formulations and *in vivo* bone-targeting properties were also investigated. Docetaxel (DTX) was selected as a model of lipophilic anticancer drug, which is first-line chemotherapy in patients with metastatic breast cancer. The bone-targeting amphiphilic MPC-based polymer can be a medical candidate for the regional chemotherapy of bone metastasis.

2. MATERIALS AND METHODS

2.1. Materials

NOF Co. (Tokyo, Japan) supplied MPC. Dichloromethane, triethylamine (TEA), and BMA were purchased from Wako Co., Ltd. (Osaka, Japan). Methacryloyl chloride, ALN, and DTX were purchased from Tokyo Chemical Industry Co., Ltd. (Tokyo, Japan). Methacryloxyethyl thiocarbamoyl rhodamine B was purchased from Polysciences, Inc. (Warrington, PA). American Type Culture Collection supplied breast cancer cells (MCF-7, MDA-MB-231, 4T1). Macrophage cells RAW264.7 and fibroblast cells L929 were purchased from DS Pharma. DMEM, Antibiotic-Antimycotic (100X), and LIVE/DEAD Viability/Cytotoxicity Kit were purchased from Thermo Fisher Scientific (Rochester, NY). Fetal bovine serum was

purchased from Biowest (Nuaille, France). Methacryloyl chloride, BMA, and triethylamine were distilled under atmospheric pressure before the experiment, and other reagents were used without further purification.

2.2. Synthesis of phospholipid polymer with alendronate group

N-Methacryloylalendronate sodium salt (NMA·Na) was prepared following Khelfallah et al.[35] The NMA was stored in −30°C, and sodium-ion was removed by passing it through Amberlite ion-exchanger resin and lyophilized before use. Conventional radical polymerization was performed to synthesize a copolymer of MPC, BMA, and NMA (PMBA). Each monomer was dissolved in methanol:water = 9:1 in a final monomer concentration of 0.5 M. After adding 2.5 mM of 2,2'-azobis(isobutyronitrile) (AIBN) as an initiator, the monomer solution was placed at 60°C for 15 h. The reaction mixture was precipitated in diethyl ether, and the remaining monomer was completely removed using a dialysis membrane (MWCO 3,500) against distilled water. PMB was also produced in the same way as described above. For biodistribution imaging, the same polymerization procedure was used to prepare rhodamine-bearing PMB and PMBA (PMB-Rho and PMBA-Rho) with an addition of a trace amount of methacryloxyethyl thiocarbamoyl

rhodamine B (M-Rho). The PMB-Rho and PMBA-Rho were dialyzed against methanol:water = 1:1. Each polymer was lyophilized after dialysis to obtain a fluffy powder. Composition ratios of MPC, BMA, and NMA were determined from ^{1}H-nuclear magnetic resonance (^{1}H-NMR) using ECZ-400 (Jeol, Tokyo, Japan) by dissolving each polymer in 50°C ethanol-d6. The composition ratio of M-Rho was measured using the 550 nm absorbance using UV-Vis spectroscopy (V-650; JASCO, Tokyo, Japan). Molecular weight and fluorescence labeling were confirmed using a gel permeation chromatography (JASCO, Tokyo, Japan), equipped with a refractive index detector, a UV/Vis detector, size-exclusion columns, Shodex SB-803 HQ, and SB-806M HQ, with a poly(ethylene glycol) standard in MeOH/water 70:30 with 50 mM LiBr. To determine the critical micelle concentration (CMC) of PMB, the fluorescence spectra of pyrene probe in the polymer aqueous solution were measured at room temperature using a fluorescence spectrophotometer (F-2500; JASCO, Tokyo, Japan), as described previously.[36]

2.3. Preparation of polymer-DTX complex

To evaluate the maximum amount of DTX encapsulated in our polymer solution, PMBA was dissolved in phosphate buffer serine (PBS) at concentrations of 50 to 200

mg/mL. The excess amount of DTX was placed and sonicated in the solution for 1 h. The mixture was centrifuged at 10,000 × g for 10 min to remove the precipitated DTX, and the supernatant was lyophilized. The same volume of the crude polymer solution was also lyophilized. By measuring the weight of dried matters, the maximum amount of the formulated DTX was calculated using the following equation:

$$S_d = (W_d - W_0)/L$$

where W_d, W_0, and L denote the dry weights of the polymer-DTX and the crude polymer solutions and the volume of supernatant, respectively.

In the assay, 0.8 mg of DTX and 50 mg of polymers (PMB or PMBA) were dissolved in 1 mL water by applying sonication for several hours. The homogeneous solutions of DTX and polymer were filtrated using a 0.45 μm syringe filter and lyophilized to form the polymer-DTX powder. The polymer was stored at 4°C and dissolved in PBS before use. For the biodistribution assay of the polymer-DTX complex, 20% of DTX was replaced by fluorescein-labeled DTX (DTX-F) in the formulation process to visualize the drug distribution. The synthesis procedure of DTX-F is described in the Supporting Information section.

2.4. Characterization of polymer-DTX complex

Zetasizer Nano ZS (Malvern Panalytical Ltd., UK) was used to measure the size and zeta potential. Polymer-DTX complex powder was dissolved in PBS at the polymer concentration of 1 mg/mL. Dynamic light scattering (DLS) was used to investigate the size distribution profile of polymer-DTX dissolved in PBS with or without divalent cations (0.90 mM $CaCl_2$ and 1.05 mM $MgCl_2$). The zeta potential of polymer-DTX dissolved in 10 mM phosphate buffer pH 7.4 was measured.

2.5. Cell cytotoxicity assay

Cytotoxicity of the polymer and the polymer-DTX complexes toward breast cancer cells (MDA-MB-231, MCF-7, and 4T1), fibroblasts (L929), and macrophages (RAW264.7) were investigated. Each cell was seeded on a 96 well plate and incubated for one day. The polymer and polymer-DTX were dissolved in PBS, and then 10 μL of the sample solutions were added to the plate to attain a final polymer concentration from 0 to 1.25 mg/mL (final DTX concentration from 0 to 25 μM). To investigate the cytotoxicity of free DTX, 1 mM DTX in ethanol was used to prepare DTX solutions. After two more days of culture, the WST-8 Cell Counting Kit (Dojindo, Tokyo, Japan) was used to estimate the number of cells. The LIVE/DEAD

Viability/Cytotoxicity Kit was used to investigate the cytotoxicity three days after the administration of PMBA-DTX according to the manufacturer's protocol.

2.6. Biodistribution assay

The rhodamine-labeled polymer was intravenously inoculated, and in vivo polymer distribution was investigated. KSN athymic nude mice (female, 6-week-old) were inoculated with 100 μL of approximately 100 mg/mL of PMB-Rho or PMBA-Rho dissolved in PBS via the tail vein. The concentrations of PMB-Rho and PMBA-Rho were adjusted so that each polymer solution had the same fluorescence intensity. Three days after injection, blood, the bone of the hind legs, and major organs (e.g., the heart, liver, spleen, lungs, pancreas, and kidneys) were harvested and analyzed using IVIS Lumina III (Caliper Life Science/PerkinElmer, USA). Tibial sagittal sections were observed using the C2 confocal microscopy system (Nikon, Japan). For the biodistribution assay of polymer-DTX complexes, 100 μL of complex solutions, composed of 50 mg/mL of PMB-Rho, PMBA-Rho, and 0.8 mg/mL DTX+DTX-F of PBS, was inoculated via a tail vein. Twenty-four hours after injection, tibial bones were harvested, and the sagittal section was observed, as described above. All the animal experiments were performed according to the

guidelines of the Animal Care and Use Committee of Matsumoto Dental University and Animal Care and Use Committee of Kansai University (authorization #1815). NIH guidelines for the care and use of laboratory animals (NIH Publication #85-23 Rev. 1985) were observed.

2.7. Statistical analysis

IC_{50} of cytotoxicity assay was evaluated by fitting the four-parameter logistic model onto the experimental survival curves. One-way ANOVA with post-hoc Tukey's test was used to perform the statistical analysis of cytotoxicity assay. Welch t-test was used to perform the statistical comparisons between fluorescence deposition of PMB and PMBA. *P*-value <0.05 was considered statistically significant.

3. RESULTS

3.1. Synthesis and characterization of polymer

As shown in Figure 1, we synthesized ALN-containing phospholipid polymer (PMBA) and PMB as a non-osteotropic reference. For the pharmacokinetic study, rhodamine-labeled PMB or PMBA (PMB-Rho and PMBA-Rho) were also

synthesized by adding a trace amount of M-Rho; the mole fraction of M-Rho was estimated from the intensity of 550 nm absorbance. Table 1 shows the molecular weight and mole fraction of each polymer. Every polymer synthesized in this study was dissolved in water. The CMC of PMBA was 8.3×10^{-4} mg/mL, which is equivalent to that of PMB reported previously.[27]

3.2. Formation of polymer-DTX complex

The amount of DTX dissolved in the PMBA/PBS solution was estimated from the dry weight of the supernatant of the polymer solution with saturated DTX. The amount of DTX in the aqueous phase was increased in tandem with an increase in PMBA concentration (see Figure 2); 5 mg of DTX was subsequently dissolved in 1 mL of 200 mg/mL PMBA solution without any turbidity. In contrast, the same amount of DTX hardly dissolved in 1 mL of PBS (see Figure 2). The maximum solubility of DTX in 50 mg/mL PMBA was 2.9 ± 1.0 mg/mL, which was 150 times higher than that in water. No precipitation was observed when the complex solution was stored for one month at 4°C (data not shown).

Next, we used the DLS measurement to find out the diameter of the polymer-DTX complex. The particle size of PMB- and PMBA-DTX complexes in PBS was 20.1 ±

0.1 and 27.0 ± 0.1 nm, respectively (see Table 2). DTX alone, solubilized with ethanol, formed aggregates with a diameter of ~100 nm (Figure S1). This implies that PMB or PMBA prevented the encapsulated DTX from forming self-assembly in the aqueous phase. PMBA-DTX powder offered good reproducibility of particle size when the powder was dissolved in PBS at the time of use for at least 1 month after the formulation (see Figure S2A). We also checked the stability of the complex dispersed in PBS at 4°C and noticed that the size and PdI hardly fluctuated in four weeks (Figure S2B). The presence of Ca^{2+} and Mg^{2+} increased the diameter of PMBA-DTX from 25.9 ± 0.6 to 35.4 ± 0.3 nm (Table S1). The measurements of zeta potential show that the introduction of the NMA unit significantly decreased the zeta potential of the polymer-DTX complex from −1.8 ± 1.0 to −11.8 ± 1.6 mV, indicating that anionic ALN was successfully introduced to the surface of the complex.

3.3. Anticancer properties of the polymer-DTX complex

Several types of cells were used to investigate the cytotoxicity of the polymer and polymer-DTX complex. Figure 3 shows the survival curves of MDA-MB-231 and L929; Figure S3 displays the survival curves of the other cells. None of the cell types exhibited cytotoxicity when they were cultured with PMBA at the concentration of

1.25 mg/mL, suggesting that PMBA is cytocompatible. The antineoplastic profiles of free DTX and PMBA-DTX were equal regardless of whether the drug was administered in a free form or was formulated with PMBA. The live/dead assay revealed that PMBA-DTX induced cell death associated with multi-nuclei formation[37] (Figure S4). Table 3 summarizes IC_{50}s in each treatment condition. In every cell type, the IC50 of PMBA-DTX and PMB-DTX was almost the same as that of free DTX, suggesting that drug formulation with our polymer did not hinder the pharmacological effects of DTX.

3.4. *In vivo* bone-targeting property of PMBA

Biodistribution of PMB or PMBA was investigated by injecting the PMB-Rho and PMBA-Rho solutions into the nude mice. Three days after injection, leg bones and major organs were harvested, and the fluorescence deposition was investigated (see Figure 4). Figure 4A shows that no significant increase in the polymer deposition of the liver, spleen, and kidneys was observed when introducing ALN moiety to PMB polymer; in contrast, the polymer deposition in the leg bones was approximately double in the PMBA-Rho group compared with the PMB-Rho group (see also Figure 4B). Histological examination of the tibiae revealed the accumulation of PMBA-Rho

on the surface of the trabecular bone (see Figure 4C). This accumulation, however, was not observed in the PMB-Rho group. We observed the line distributions of the PMBA-DTX complex bound on the trabecular bones accompanied by higher accumulation of DTX-F distributed on the bone surface (see Figure 5 D–F). In contrast, the accumulations of PMB-DTX were not prominent compared with those of the PMBA-DTX group (see Figure 5 A–C). These results suggest that PMBA is a potential polymer for the osteotropic delivery of DTX.

4. DISCUSSION

In chemotherapy for breast or prostate cancers, the current strategy involves an adjuvant/neoadjuvant medication in early resectable stages, or a palliative remedy for the later metastatic stages. Bone-residing chemotherapy is a great option to achieve a clinical response to the suppression of the metastatic bone tumor. In this study, the amphiphilic and osteotropic copolymer bearing MPC was produced; this copolymer offers the hydrophobic pocket to encapsulate DTX and deliver the drug to bone tissues. Konno et al. proposed that amphiphilic MPC polymer containing 30% of BMA can improve the solubility of paclitaxel in the aqueous phase for at least 1

mg/mL.[27] This principle was applied to design our bone-targeting phospholipid polymers, and the PMBA aqueous solution (50 mg/mL) could make >2 mg/mL of the DTX dissolved in the aqueous phase (Figure 2) to form nanoparticles with a diameter of <30 nm (Table 2). Particle size is a key element for efficient transportation across fenestrated sinusoidal capillary in the bone marrow. It ensures that the non-endogenous particles in a diameter of 60 nm or less can spread to the bone marrow via the phago-endocytic route;[38] our PMBA-DTX complex conformed to this requirement. Moreover, DTX entrapped by PMBA gave the same antineoplastic profile as free DTX (Figure 3 and Table 3), which is also comparable with previous reports.[32],[39] The introduction of ALN on the surface of nanoparticles was identified by the decreasing zeta potential arising from anionic NMA (Table 2). The introduction of ALN also increased the size of PMBA-DTX complex in the presence of Ca^{2+} and Mg^{2+} (Table S1), which is because ALN moiety have strong affinity to divalent cations to form electrostatic cross-links between the nanoparticles in a similar manner reported by Nishiguchi et al.[40]; however, the size of whole assembly is still <40 nm and small enough for bone-targeting drug transportation. The fluorescence biodistribution assays revealed the osteotropic property of PMBA in both its free polymer form (Figure 4) and its complex form (Figure 5).

ALN-containing macromolecules tend to accumulate in the sites of bone metastasis because of accelerated bone remodeling,[11] with the bone-targeted biodistribution of PMBA presumptively becoming more prominent in a metastatic site. Collectively, PMBA is a potential osteotropic carrier for bone-residing chemotherapy by encapsulating hydrophobic DTX.

Ethanol-free excipients are highly expected to formulate taxoid drugs to avoid several side effects, such as hypersensitivity reactions (HSRs) and alcohol sensitivity. For example, ethanol-free paclitaxel formulated with albumin (ABI-007 or Abraxane) was reported to completely eliminate severe HSRs despite the absence of premedication.[41] Other research groups have also reported that PMB is an alternative ethanol-free agent for formulating paclitaxel because PMB-paclitaxel complex causes neither skin ulcer at the site of injection[39] nor an intolerable transient increase in alanine aminotransferase (ALT).[42] Our data indicated that DTX was successfully formulated by PMBA without any ethanol (Figure 2), and PMBA did not show any cytotoxic against fibroblast and macrophage cells as PMB did (Figure 3). Taken together, PMBA can act as an effective formulating agent to avoid solvent-based side effects.

Bone-targeting delivery is also able to suppress non-bone-related side effects, such as peripheral neuropathy, fluid retentions, or left ventricular dysfunction, which are parts of mortal causes of high-dose chemotherapy.[9],[43] In the biodistribution assay, no significant increase in polymers accumulation was observed in any organs except for the bones (Figure 4A), suggesting that the introduction of ALN moiety will not induce any unintended drug accumulation. However, it should be noted that our current bone-targeting strategy offers little improvement in avoiding bone marrow suppression, and more improvements will be required to deal with this problem.[43] One possible solution involves immobilizing cancer-targeting functional groups related to PMBA to deliver the drug to the tumor cell after reaching the bone-metastatic area. Another solution involves using alternative antineoplastic agents with milder bone marrow suppression compared with taxoid drugs, such as lapatinib, gemcitabine, or methotrexate.

The tolerance of PMBA needs to be investigated for further study. ALN is a class of BPs that are commonly used as antiresorptive agents to treat bone diseases that involve excessive bone resorption, such as osteoporosis, Paget's disease, and bone metastasis.[44] Because of the strong suppression of bone turnover, exceeding the administration of BPs can induce atypical fractures caused by microdamage

accumulation.[45] No significant cytotoxicity was observed when L929 was cultured in 1,250 μg/mL of PMBA, which corresponds to 290 μM ANL (Figure 3B); however, ≥100 μM nitrogen-containing BPs have been reported to be toxic to several fibroblast cells.[46] This may be because the cytotoxicity of ALN was reduced by the immobilization on MPC polymer in a manner similar to a reduced toxicity of drugs immobilized on HPMA polymer, reported by Segal et al. in [13]. The research group also performed a maximum tolerated dose test in which mice were intravenously injected five times with 9.5 mg/kg of ALN conjugated with HPMA polymer, causing no significant loss of body weight or a decrease in the number of white blood cells.[11] By this standard, up to 6.5 mg/kg of DTX can be administered using our system, and this concentration is high enough for the evaluation of antitumor activities in mice. However, for human application, the amount of ALN introduced in PMBA still requires further investigation. For instance, in the conventional DTX chemotherapy, 3.4 g of polysorbate 80 is needed to formulate ≤75 mg/m^2 of DTX to a medium-built person with an average body surface area of 1.7 m^2.[47] To formulate the same volume of DTX (130 mg), 3.25 g of PMBA is required, which is almost equivalent to the amount of polysorbate 80. With this assumption, the amount of ALN administered in one intravenous infusion will be 188 mg/dose,

which provides 47 times higher blood concentration of BPs than the recommended dose (4 mg/dose) for preventing skeletal complications related to the bone metastases prostate cancer.[48] Moreover, the extent of the effect of PMBA on osteoblasts and osteoclasts is still unclear, calling for further investigations into the pharmacological effects of PMBA on bone metabolism. If PMBA has an intolerable adverse effect on bone turnovers, other bone-targeting moieties, such as tetracycline,[49] acidic oligopeptides,[50] and anionic polyphosphoesters,[36],[51] may have to be considered.

Since this is a preliminary report, further optimization will be required to maximize the deposition and the anticancer property of our bone-targeting system. The biodistribution of PMBA was investigated only three days after injection; nonetheless, little is known about the pharmacokinetic process of PMBA and PMBA-DTX complexes. The hydrodynamic diameter and concentration of targeting ligand are key factors in maximizing the deposition of drugs in the affected area.[19] Pan et al. compared the bone deposition of HPMA, bearing different ratios of ALN moiety (0, 1.5, 8.5 mol%), with a molecular weight of 90 kDa whose hydrodynamic volume was equivalent to our polymers.[52] In the report, the highest bone deposition was obtained using HPMA with 1.5% ALN moiety, which indicates that there may exist an optimized proportion of ALN. Many researchers have reported that an

increase in ALN moiety and hydrodynamic diameter will lead to the deposition of osteotropic polymers in the liver and spleen via the reticuloendothelial system. In this study, however, no significant increase in the polymer deposition of the liver and spleen was observed when introducing ALN moiety to PMB polymer, and this may be caused by the stealth property of MPC moiety of PMBA. The releasing kinetics of DTX from PMBA-DTX complex after the administration is another issue to be addressed. Soma et al. reported that PMB-encapsulation promote the infiltration of paclitaxel into a tumor tissue up to 24 h after administration[29], suggesting that the PMB-paclitaxel complex keeps the structure during the transportation. On the other hand, Mu et al. reported the drug-release from PMB-paclitaxel complex takes place in the presence of plasma proteins due to the transfer of paclitaxel from the complex to the proteins[53]. Further research is needed to examine which situation is more likely to occur in our system.

5. CONCLUSIONS

The biodistribution assay of our phospholipid polymer revealed that the introduction of bone-targeting moiety selectively improved the polymer

accumulation in bones. DTX formulated with PMBA is a potential drug agent to provide a high-dose condition in the metastatic bone environment. Our bone-targeting phospholipid polymer did not associate itself with any remarkable toxicity in this *in vitro* and *in vivo* study. The next step will involve using a bone metastasis mouse model to probe the detailed hemodynamic and pathological responses of bone metastasis of PMBA-DTX.

ACKNOWLEDGMENTS

This work was supported by the Grant-in-Aid for Challenging Research (Exploratory) (No. 18K19656) from the Japan Society for the Promotion of Science, MEXT Private University Research Branding Project, and by Kansai University Fund for Supporting Young Scholars, 2018. We thank Associate Professor Shin-ichi Yusa of University of Hyogo for his advice about NMR measurement of PMBA. We thank Associate Professor Issey Osaka of Toyama Prefectural University for ESI/MS measurement of DTX-F.

.

REFERENCES

1. Hori M, Matsuda T, Shibata A, Katanoda K, Sobue T, Nishimoto H. Cancer incidence and incidence rates in Japan in 2009: a study of 32 population-based cancer registries for the Monitoring of Cancer Incidence in Japan (MCIJ) project. Jpn J Clin Oncol 2015;45:884–891.

2. Ferlay J, Soerjomataram I, Dikshit R, Eser S, Mathers C, Rebelo M, Parkin DM, Forman D, Bray F. Cancer incidence and mortality worldwide: Sources, methods and major patterns in GLOBOCAN 2012. Int J Cancer 2015;136:E359–386.

3. Schroeder A, Heller DA, Winslow MM, Dahlman JE, Pratt GW, Langer R, Jacks T, Anderson DG. Treating metastatic cancer with nanotechnology. Nat Rev Cancer 2012;12:39–50.

4. Nørgaard M, Jensen AØ, Jacobsen JB, Cetin K, Fryzek JP, Sørensen HT. Skeletal Related Events, Bone Metastasis and Survival of Prostate Cancer: A Population Based Cohort Study in Denmark (1999 to 2007). J Urol 2010;184:162–167.

5. Amat S, Bougnoux P, Penault-Llorca F, Fétissof F, Curé H, Kwiatkowski F, Achard JL, Body G, Dauplat J, Chollet P. Neoadjuvant docetaxel for operable

breast cancer induces a high pathological response and breast-conservation rate. Br J Cancer 2003;88:1339–1345.

6. Zhao B, Yerram NK, Gao T, Dreicer R, Klein EA. Long-term survival of patients with locally advanced prostate cancer managed with neoadjuvant docetaxel and radical prostatectomy. Urol Oncol 2015;33:164.e19-164.e23.

7. Sledge GW. Curing Metastatic Breast Cancer. J Oncol Pract. 2016;12:6–10.

8. Dong L, Zieren RC, Xue W, de Reijke TM, Pienta KJ. Metastatic prostate cancer remains incurable, why? Asian J Urol 2019;6:26–41.

9. Crump M, Gluck S, Tu D, Stewart D, Levine M, Kirkbride P, Dancey J, O'Reilly S, Shore T, Couban S, Girouard C, Marlin S, Shepherd L, Pritchard KI. Randomized trial of high-dose chemotherapy with autologous peripheral-blood stem-cell support compared with standard-dose chemotherapy in women with metastatic breast cancer: NCIC MA.16. J Clin Oncol 2008;26:37–43.

10. Farquhar C, Basser R, Hetrick S, Lethaby A, Marjoribanks J. High dose chemotherapy and autologous bone marrow or stem cell transplantation versus conventional chemotherapy for women with metastatic breast cancer. Cochrane database Syst Rev 2003;CD003142.

11. Miller K, Eldar-Boock A, Polyak D, Segal E, Benayoun L, Shaked Y, Satchi-Fainaro R. Antiangiogenic Antitumor Activity of HPMA Copolymer–Paclitaxel–Alendronate Conjugate on Breast Cancer Bone Metastasis Mouse Model. Mol Pharm 2011;8:1052–1062.

12. Miller K, Erez R, Segal E, Shabat D, Satchi-Fainaro R. Targeting bone metastases with a bispecific anticancer and antiangiogenic polymer-alendronate-taxane conjugate. Angew Chemie - Int Ed 2009;48:2949–2954.

13. Segal E, Pan H, Ofek P, Udagawa T, Kopečková P, Kopeček J, Satchi-Fainaro R. Targeting Angiogenesis-Dependent Calcified Neoplasms Using Combined Polymer Therapeutics. PLoS One 2009;4:e5233.

14. Ye WL, Zhao YP, Li HQ, Na R, Li F, Mei QB, Zhao MG, Zhou SY. Doxorubicin-poly (ethylene glycol)-alendronate self-assembled micelles for targeted therapy of bone metastatic cancer. Sci Rep 2015;5:1–19.

15. Swami A, Reagan MR, Basto P, Mishima Y, Kamaly N, Glavey S, Zhang S, Moschetta M, Seevaratnam D, Zhang Y, Liu J, Memarzadeh M, Wu J, Manier S, Shi J, Bertrand N, Lu ZN, Nagano K, Baron R, Sacco A, Roccaro AM, Farokhzad OC, Ghobrial IM. Engineered nanomedicine for myeloma and bone

microenvironment targeting. Proc Natl Acad Sci 2014;111:10287–10292.

16. Chen H, Li G, Chi H, Wang D, Tu C, Pan L, Zhu L, Qiu F, Guo F, Zhu X. Alendronate-conjugated amphiphilic hyperbranched polymer based on boltorn H40 and poly(ethylene glycol) for bone-targeted drug delivery. Bioconjug Chem 2012;23:1915–1924.

17. Choi S-W, Kim J-H. Design of surface-modified poly(D,L-lactide-*co*-glycolide) nanoparticles for targeted drug delivery to bone. J Control Release 2007;122:24–30.

18. Wang D, Sima M, Mosley RL, Davda JP, Tietze N, Miller SC, Gwilt PR, Kopečková P, Kopeček J. Pharmacokinetic and Biodistribution Studies of a Bone-Targeting Drug Delivery System Based on *N*-(2-Hydroxypropyl)methacrylamide Copolymers. Mol Pharm 2006;3:717–725.

19. Low SA, Kopeček J. Targeting polymer therapeutics to bone. Adv Drug Deliv Rev 2012;64:1189–1204.

20. Wang H, Liu X, Wang Y, Chen Y, Jin Q, Ji J. Doxorubicin conjugated phospholipid prodrugs as smart nanomedicine platforms for cancer therapy. J Mater Chem B 2015;3:3297–3305.

21. Kierstead PH, Okochi H, Venditto VJ, Chuong TC, Kivimae S, Fréchet JMJ, Szoka FC. The effect of polymer backbone chemistry on the induction of the accelerated blood clearance in polymer modified liposomes. J Control Release 2015;213:1–9.

22. Ishihara K, Ueda T, Nakabayashi N. Preparation of Phospholipid Polylners and Their Properties as Polymer Hydrogel Membranes. Polym J 1990;22:355–360.

23. Sugiyama K, Mitsuno S, Shiraishi K. Adsorption of protein on the surface of thermosensitive poly(methyl methacrylate) microspheres modified with the *N*-(2- hydroxypropyl)methacrylamide and 2- (methacryloyloxy)ethyl phosphorylcholine moieties. J Polym Sci Part A Polym Chem 1997;35:3349–3357.

24. Ishihara K, Chen W, Liu Y, Tsukamoto Y, Inoue Y. Cytocompatible and multifunctional polymeric nanoparticles for transportation of bioactive molecules into and within cells. Sci Technol Adv Mater 2016;17:300–312.

25. Jin Q, Chen Y, Wang Y, Ji J. Zwitterionic drug nanocarriers: A biomimetic strategy for drug delivery. Colloids Surfaces B Biointerfaces 2014;124:80–86.

26. Ishihara K, Iwasaki Y, Nakabayashi N. Polymeric Lipid Nanosphere Consisting

of Water-Soluble Poly(2-methacryloyloxyethyl phosphorylcholine-*co*-*n*-butyl methacrylate). Polym J 1999;31:1231–1236.

27. Konno T, Watanabe J, Ishihara K. Enhanced solubility of paclitaxel using water-soluble and biocompatible 2-methacryloyloxyethyl phosphorylcholine polymers. J Biomed Mater Res A 2003;65:209–214.

28. Miyata R, Ueda M, Jinno H, Konno T, Ishihara K, Ando N, Kitagawa Y. Selective targeting by preS1 domain of hepatitis B surface antigen conjugated with phosphorylcholine-based amphiphilic block copolymer micelles as a biocompatible, drug delivery carrier for treatment of human hepatocellular carcinoma with paclitaxel. Int J Cancer 2009;124:2460–2467.

29. Soma D, Kitayama J, Konno T, Ishihara K, Yamada J, Kamei T, Ishigami H, Kaisaki S, Nagawa H. Intraperitoneal administration of paclitaxel solubilized with poly(2-methacryloxyethyl phosphorylcholine-co *n*-butyl methacrylate) for peritoneal dissemination of gastric cancer. Cancer Sci 2009;100:1979–1985.

30. Tamura K, Kikuchi E, Konno T, Ishihara K, Matsumoto K, Miyajima A, Oya M. Therapeutic effect of intravesical administration of paclitaxel solubilized with poly(2-methacryloyloxyethyl phosphorylcholine-co-*n*-butyl methacrylate) in an

orthotopic bladder cancer model. BMC Cancer 2015;15:317.

31. Goto Y, Matsuno R, Konno T, Takai M, Ishihara K. Artificial cell membrane-covered nanoparticles embedding quantum dots as stable and highly sensitive fluorescence bioimaging probes. Biomacromolecules 2008;9:3252–3257.

32. Chiba N, Ueda M, Shimada T, Jinno H, Watanabe J, Ishihara K, Kitajima M. Novel immunosuppressant agents targeting activated lymphocytes by biocompatible MPC polymer conjugated with interleukin-2. Eur Surg Res 2007;39:103–110.

33. Nishizawa K, Konno T, Takai M, Ishihara K. Bioconjugated phospholipid polymer biointerface for enzyme-linked immunosorbent assay. Biomacromolecules 2008;9:403–407.

34. Otaka A, Kitagawa K, Nakaoki T, Hirata M, Fukazawa K, Ishihara K, Mahara A, Yamaoka T. Label-Free Separation of Induced Pluripotent Stem Cells with Anti-SSEA-1 Antibody Immobilized Microfluidic Channel. Langmuir 2017;33:1576–1582.

35. Kachbi Khelfallah S, Monteil M, Deschamp J, Gager O, Migianu-Griffoni E,

Lecouvey M. Synthesis of novel polymerizable molecules bearing bisphosphonate. Org Biomol Chem. 2015;13:11382–11392.

36. Hirano Y, Iwasaki Y. Bone-specific poly(ethylene sodium phosphate)-bearing biodegradable nanoparticles. Colloids Surfaces B Biointerfaces 2017;153:104–110.

37. Hernández-Vargas H, Palacios J, Moreno-Bueno G. Molecular profiling of docetaxel cytotoxicity in breast cancer cells: Uncoupling of aberrant mitosis and apoptosis. Oncogene 2007;26:2902–2913.

38. Sarin H. Physiologic upper limits of pore size of different blood capillary types and another perspective on the dual pore theory of microvascular permeability. J Angiogenes Res 2010;2:14.

39. Wada M, Jinno H, Ueda M, Ikeda T, Kitajima M, Konno T, Watanabe J, Ishihara K. Efficacy of an MPC-BMA co-polymer as a nanotransporter for paclitaxel. Anticancer Res 2007;27:1431–1435.

40. Nishiguchi A, Taguchi T. Osteoclast-Responsive, Injectable Bone of Bisphosphonated-Nanocellulose that Regulates Osteoclast/Osteoblast Activity for Bone Regeneration. Biomacromolecules 2019;20:1385-1393.

41. Gradishar WJ, Tjulandin S, Davidson N, Shaw H, Desai N, Bhar P, Hawkins M, O'Shaughnessy J. Phase III trial of nanoparticle albumin-bound paclitaxel compared with polyethylated castor oil-based paclitaxel in women with breast cancer. J Clin Oncol 2005;23:7794–7803.

42. Kamei T, Kitayama J, Yamaguchi H, Soma D, Emoto S, Konno T, Ishihara K, Ishigami H, Kaisaki S, Nagawa H. Spatial distribution of intraperitoneally administrated paclitaxel nanoparticles solubilized with poly (2-methacryloxyethyl phosphorylcholine-co *n*-butyl methacrylate) in peritoneal metastatic nodules. Cancer Sci 2011;102:200–205.

43. Markman M. Managing taxane toxicities. Support Care Cancer 2003;11:144–147.

44. Luckman SP, Hughes DE, Coxon FP, Graham R, Russell G, Rogers MJ. Nitrogen-containing bisphosphonates inhibit the mevalonate pathway and prevent post-translational prenylation of GTP-binding proteins, including Ras. J Bone Miner Res 1998;13:581–589.

45. Saito M, Mori S, Mashiba T, Komatsubara S, Marumo K. Collagen maturity, glycation induced-pentosidine, and mineralization are increased following 3-year treatment with incadronate in dogs. Osteoporos Int 2008;19:1343–1354.

46. Tanaka Y, Nagai Y, Dohdoh M, Oizumi T, Ohki A, Kuroishi T, Sugawara S, Endo Y. In vitro cytotoxicity of zoledronate (nitrogen-containing bisphosphonate: NBP) and/or etidronate (non-NBP) in tumour cells and periodontal cells. Arch Oral Biol 2013;58:628–637.

47. Sacco JJ, Botten J, Macbeth F, Bagust A, Clark P. The average body surface area of adult cancer patients in the UK: A multicentre retrospective study. PLoS One 2010;5:1–6.

48. Saad F, Gleason DM, Murray R, Tchekmedyian S, Venner P, Lacombe L, Chin JL, Vinholes JJ, Goas JA, Zheng M. Long-term efficacy of zoledronic acid for the prevention of skeletal complications in patients with metastatic hormone-refractory prostate cancer. J Natl Cancer Inst 2004;96:879–882.

49. Pierce WM, Waite LC. Bone-Targeted Carbonic Anhydrase Inhibitors: Effect of a Proinhibitor on Bone Resorption in Vitro. Exp Biol Med 1987;186:96–102.

50. Wang D, Miller SC, Shlyakhtenko LS, Portillo AM, Liu XM, Papangkorn K, Kopečková P, Lyubchenko Y, Higuchi WI, Kopeček J. Osteotropic peptide that differentiates functional domains of the skeleton. Bioconjug Chem 2007;18:1375–1378.

51. Iwasaki Y, Yokota A, Otaka A, Inoue N, Yamaguchi A, Yoshitomi T, Yoshimoto K, Neo M. Bone-targeting poly(ethylene sodium phosphate). Biomater Sci 2018;6:91–95.

52. Pan H, Sima M, Kopečková P, Wu K, Gao S, Liu J, Wang D, Miller SC, Kopeček J. Biodistribution and Pharmacokinetic Studies of Bone-Targeting *N*-(2-Hydroxypropyl)methacrylamide Copolymer−Alendronate Conjugates. Mol Pharm 2008;5:548–558.

53. Mu M, Konno T, Inoue Y, Ishihara K. Solubilization of poorly water-soluble compounds using amphiphilic phospholipid polymers with different molecular architectures. Colloids Surfaces B Biointerfaces 2017;158:249–256.

FIGURES

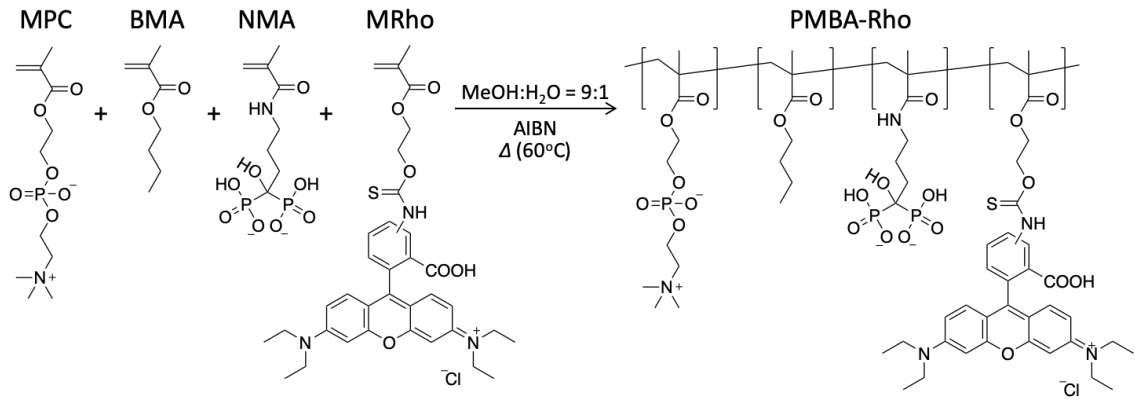

Figure 1. Synthetic scheme of PMBA-Rho.

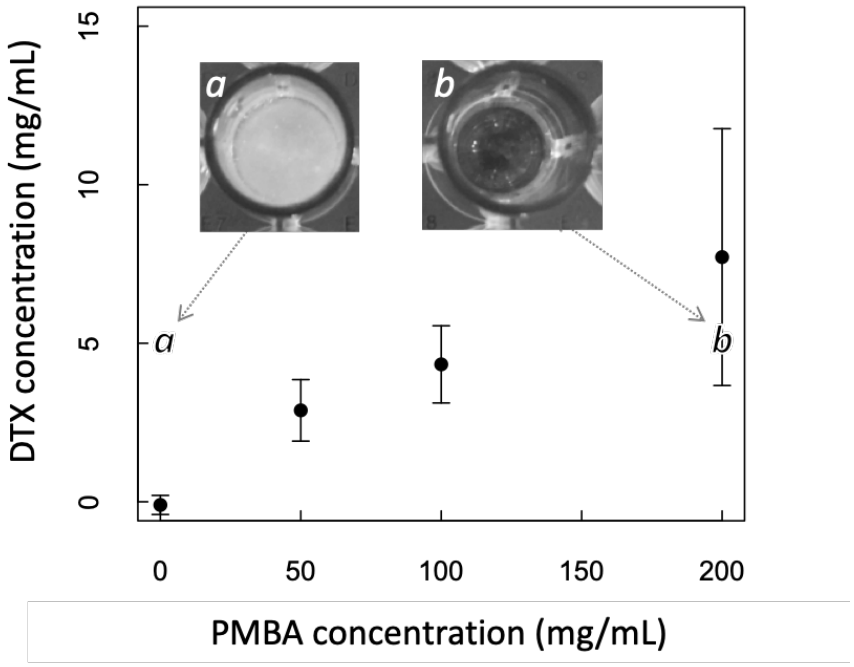

Figure 2. Solubility curve of DTX in the PMBA solution. The picture of DTX placed (a) in PBS and (b) in the PMBA solution. The concentrations of DTX and PMBA polymer are 5 and 200 mg/mL, respectively. $N = 3$, mean ± SD.

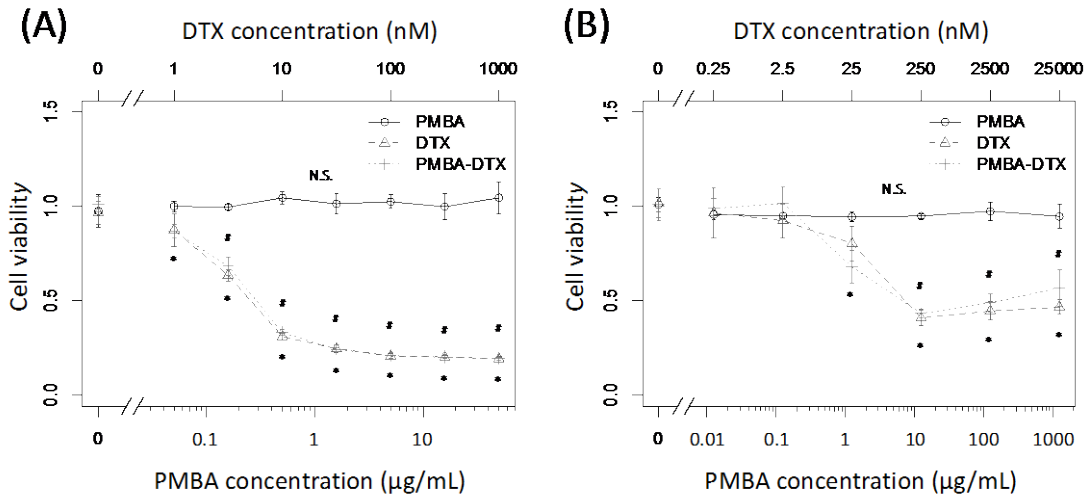

Figure 3. Cytotoxicity profiles of (A) MDA-MB-231 and (B) L929 with the administration of PMBA and PMBA-DTX. PMBA alone induced no cytotoxicity in both cell types (circle). The patterns for PMBA-DTX (cross) and free DTX (triangle) are equal, indicating that the complex formation did not hamper the pharmacological effects of DTX. N = 3, mean ± SD. Asterisk, significant difference in PMBA-DTX compared with the additive-free control (*p-value <0.05); hash, significant difference in DTX compared with the additive-free control ($^{\#}p$-value <0.05); N.S., no significant change in PMBA (p-value >0.05).

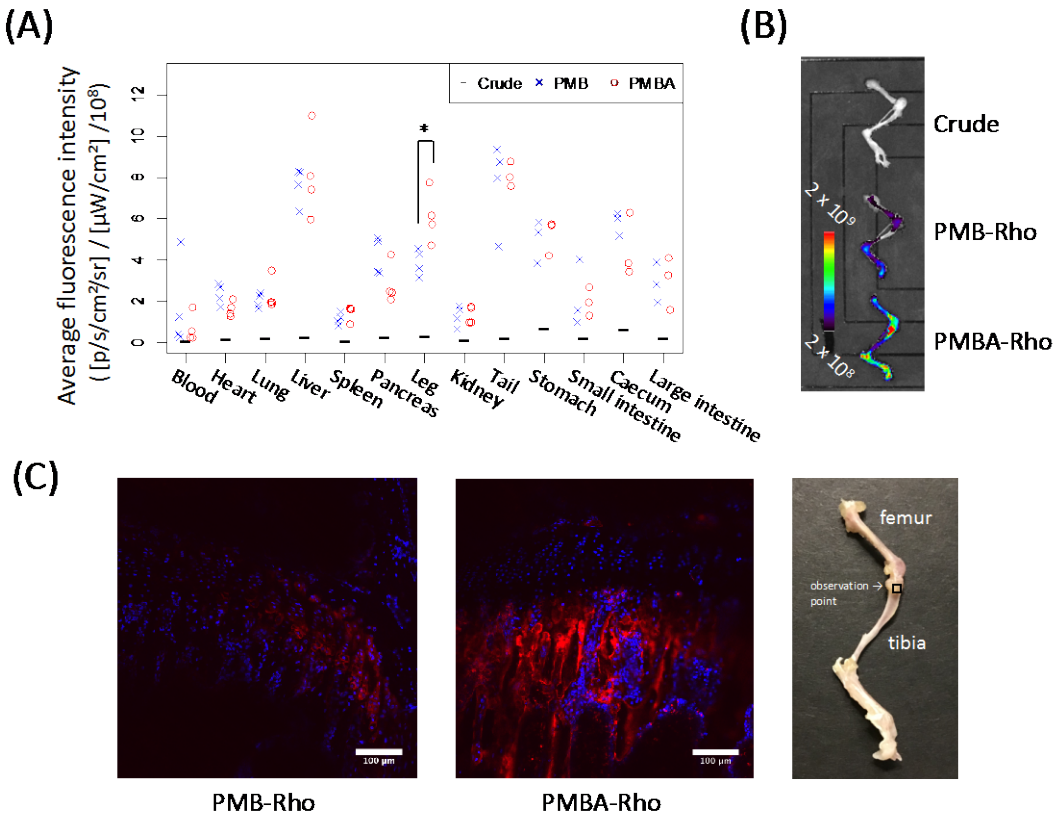

Figure 4. The biodistribution of PMB-Rho or PMBA-Rho three days after intravenous injection. (A) The intensity of PMB-Rho (cross) or PMBA-Rho (circle) accumulated in each organ was measured using interest analysis; *p-value <0.05 in the Welch t-test. (B) An *ex vivo* fluorescence image of leg bone. (C) A sagittal section of the proximal end of the tibia was observed using confocal microscopy. Nuclei (blue) and rhodamine-labeled polymer (red) were excited at 405 nm (emission collected from 417 to 477 nm) and at 561 nm (emission collected from 571 to 1000 nm), respectively. Magnification 20×. Bar = 100 μm.

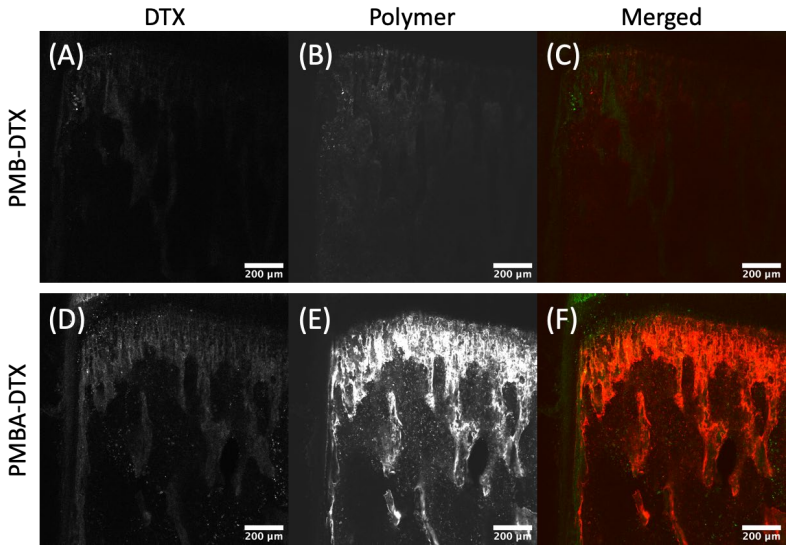

Figure 5. Confocal microscopy of the sagittal section of the proximal end of the tibia, harvested from mice 24 h after intravenous injection of PMB-DTX (A–C) and PMBA-DTX (D–F). DTX-F (A, D, green in C and F) and rhodamine-labeled polymer (B, E, red in C and F) were excited at 405 nm (emission collected from 417 to 477 nm) and at 561 nm (emission collected from 571 to 1000 nm), respectively. Magnification 10×. Bar = 200 µm.